



THE UNIVERSITY *of* EDINBURGH

Edinburgh Research Explorer

Fast explicit algorithms for Hamiltonian numerical integration

Citation for published version:

Bilbao, S & Ducceschi, M 2022, Fast explicit algorithms for Hamiltonian numerical integration. in *Proceedings of the 2020 European Nonlinear Dynamics Conference*. Lyon, France, 10th European Nonlinear Dynamics Conference, Lyon, France, 5/07/20.

Link:

[Link to publication record in Edinburgh Research Explorer](#)

Document Version:

Publisher's PDF, also known as Version of record

Published In:

Proceedings of the 2020 European Nonlinear Dynamics Conference

General rights

Copyright for the publications made accessible via the Edinburgh Research Explorer is retained by the author(s) and / or other copyright owners and it is a condition of accessing these publications that users recognise and abide by the legal requirements associated with these rights.

Take down policy

The University of Edinburgh has made every reasonable effort to ensure that Edinburgh Research Explorer content complies with UK legislation. If you believe that the public display of this file breaches copyright please contact openaccess@ed.ac.uk providing details, and we will remove access to the work immediately and investigate your claim.



Fast Explicit Algorithms for Hamiltonian Numerical Integration

Stefan Bilbao* and Michele Ducceschi†

*Acoustics and Audio Group, University of Edinburgh, Edinburgh UK

†Department of Industrial Engineering, University of Bologna, Bologna, Italy

Summary. Numerical integration methods for Hamiltonian systems are of importance across many disciplines, including musical acoustics, where many systems of interest are very nearly lossless. Of particular interest are methods possessing a conserved pseudoenergy. Though most such methods have an implicit character, an explicit method was proposed recently by Marazzato et al. The proposed method relies on a continuous integration which must be performed exactly in order for the conservation property to hold—as a result, it holds only approximately under numerical quadrature. Here, we show an explicit scheme for Hamiltonian integration, with a different choice of pseudoenergy, which is exactly conserved. Most importantly, a fast implementation is possible through the use of structured matrix inversion, and in particular Sherman Morrison inversion of the rank 1 perturbation of a matrix. Applications to the cases of fully nonlinear string vibration, and to the Föppl-von Kármán system describing large amplitude plate vibration are illustrated. Computation times are on par with the simplest non-conservative methods, such as Störmer integration.

Introduction

Numerical integration methods that preserve an invariant energy-like quantity (or pseudoenergy) form part of the larger family of geometric numerical integration methods [1]. In a recent article [2], an explicit method for Hamiltonian integration was presented, incorporating a conserved pseudo-energy. The method relies, however, on a continuous integration, meaning that pseudoenergy is only preserved approximately due to discretisation error.

New methods, relying on potential energy quadratisation are suitable for systems under more restrictive conditions (non-negativity of the potential energy) [3]. In this paper, it will be shown that such methods can be made fully explicit through structured matrix inversion techniques, and in particular, Sherman Morrison inversion for matrices under a rank-1 perturbation. This allows for extremely efficient numerical solution, while maintaining pseudo-energy conservation to machine accuracy. In particular, no full linear system solutions are required to advance the solution, in contrast with what has been presented for other methods based on quadratisation [3]. Numerical stability is ensured, through the enforced non-negativity of the numerical energy.

Two examples, that of fully nonlinear string vibration, and the nonlinear vibration of a thin plate according to the Föppl-von Kármán system are presented, illustrating good numerical behaviour, and acceleration relative to other energy conserving designs. In a companion paper [4], the realistic case of piano string vibration will be broached in detail, as well as the very important topic of the possibility of the shift in the potential energy of the system in order to improve convergence rates.

Hamiltonian Systems and Quadratisation

Consider a Hamiltonian $H(\mathbf{p}, \mathbf{q})$ of the form:

$$H(\mathbf{p}, \mathbf{q}) = \frac{1}{2} \mathbf{p}^T \mathbf{M}^{-1} \mathbf{p} + V(\mathbf{q}) \quad (1)$$

Here, $\mathbf{p}(t)$ and $\mathbf{q}(t)$ are $N \times 1$ vectors and functions of time $t \geq 0$. $\mathbf{M} > 0$ is a constant symmetric $N \times N$ mass matrix (for simplicity constrained here to be diagonal). \mathbf{p} and \mathbf{q} have the interpretation of generalized momentum and position, respectively. Hamilton's equations [5] follow as

$$\mathbf{M} \dot{\mathbf{q}} - \mathbf{p} = \mathbf{0} \quad \dot{\mathbf{p}} + \nabla V = \mathbf{0} \quad (2)$$

Here, ∇ is the gradient with respect to \mathbf{q} , and dots indicate time differentiation. Equations (2) require initialisation through $\mathbf{p}(0) = \mathbf{p}_0$ and $\mathbf{q}(0) = \mathbf{q}_0$.

Under the constraint that $V \geq 0$, one may write, using $\psi = \sqrt{2V}$,

$$H(\mathbf{p}, \mathbf{q}) = \frac{1}{2} \mathbf{p}^T \mathbf{M}^{-1} \mathbf{p} + \frac{1}{2} \psi^2 \quad (3)$$

Now, Hamilton's equations may be written as

$$\mathbf{M} \dot{\mathbf{q}} - \mathbf{p} = \mathbf{0} \quad \dot{\mathbf{p}} + \psi \mathbf{g} = \mathbf{0} \quad \dot{\psi} = \mathbf{g}^T \dot{\mathbf{q}} \quad (4)$$

where the intermediate variable $\mathbf{g} \triangleq \nabla \psi$ has been introduced. Such a quadratisation of the potential energy has appeared recently in the context of port-Hamiltonian methods [6, 7], and in finite difference schemes modeling collisions [8] and for string vibration under nonlinear conditions [9], and in other areas such as the modeling of binary fluids [10].

Notice that the form of the Hamiltonian in (1) is not the most general available, and thus some restrictions are placed on the range of applications in this paper. First, the energy is quadratic in the momentum \mathbf{p} , and thus the resulting dynamics are linear in \mathbf{p} —a very common choice across many application areas in structural vibration. Second, the potential energy V is constrained to be non-negative—a condition also common in structural vibration, but violated in other systems, such as the N -body problem under a gravitational potential. The numerical stability property of the methods presented in this paper hinges on these two restrictions.

A Pseudo-energy Conserving Explicit Fast Algorithm

Consider now a time-interleaved scheme for the dynamical system in (4):

$$\mathbf{q}^{n+1} = \mathbf{q}^n + k\mathbf{M}^{-1}\mathbf{p}^{n+\frac{1}{2}} \quad \mathbf{p}^{n+\frac{1}{2}} = \mathbf{p}^{n-\frac{1}{2}} - \frac{k}{2} \left(\psi^{n+\frac{1}{2}} + \psi^{n-\frac{1}{2}} \right) \mathbf{g}^n \quad \psi^{n+\frac{1}{2}} = \psi^{n-\frac{1}{2}} + \frac{1}{2} (\mathbf{g}^n)^T (\mathbf{q}^{n+1} - \mathbf{q}^{n-1}) \quad (5)$$

It is defined for discrete time sequences \mathbf{q}^n , $\mathbf{p}^{n+\frac{1}{2}}$ and $\psi^{n+\frac{1}{2}}$, for integer n , representing approximations at times $t = nk$ to $\mathbf{q}(t)$ and at times $t = (n + \frac{1}{2})k$ to $\mathbf{p}(t)$ and $\psi(t)$. Here, k is the time step. \mathbf{g}^n may be calculated explicitly by evaluating the analytic gradient of ψ at \mathbf{q}^n . The scheme (5) conserves the following pseudoenergy:

$$H^{n+\frac{1}{2}} = \frac{1}{2} \left(\mathbf{p}^{n+\frac{1}{2}} \right)^T \mathbf{M}^{-1} \mathbf{p}^{n+\frac{1}{2}} + \frac{1}{2} \left(\psi^{n+\frac{1}{2}} \right)^2 = \text{constant} \quad (6)$$

and thus $H^{n+\frac{1}{2}} = H$ is a constant for all n . It is non-negative, implying unconditional stability, as well as bounds on $\mathbf{p}^{n+\frac{1}{2}}$ for all n . In particular, (6) above implies that

$$\|\mathbf{p}^{n+\frac{1}{2}}\| \leq \sqrt{\frac{2H}{\lambda_{\max}(\mathbf{M})}} \quad (7)$$

where $\lambda_{\max}(\mathbf{M})$ is the maximum eigenvalue of \mathbf{M} , and $\|\mathbf{p}^{n+\frac{1}{2}}\|$ is the L_2 norm of $\mathbf{p}^{n+\frac{1}{2}}$.

Fast Update

At first glance, the updates (5) appear to be implicit, thus requiring an iterative solver at each time step. This is not the case, however. Given \mathbf{q}^n , \mathbf{q}^{n-1} and $\psi^{n-\frac{1}{2}}$ (as well as \mathbf{g}^n , determined directly from \mathbf{q}^n), they may be consolidated into an update of the form

$$\mathbf{A}^n \mathbf{q}^{n+1} = \mathbf{b}^n \quad \mathbf{A}^n = \mathbf{M} + \frac{k^2}{4} \mathbf{g}^n (\mathbf{g}^n)^T \quad \mathbf{b}^n = 2\mathbf{M}\mathbf{q}^n - k^2 \mathbf{g}^n \psi^{n-\frac{1}{2}} - \left(\mathbf{M} - \frac{k^2}{4} \mathbf{g}^n (\mathbf{g}^n)^T \right) \mathbf{q}^{n-1} \quad (8)$$

This update, which does not require iterative solvers, can be simplified by exploiting the structure of \mathbf{A}^n , which is a rank one perturbation of a matrix with an easily computed explicit inverse (\mathbf{M}). Using the Sherman-Morrison formula [11],

$$(\mathbf{A}^n)^{-1} = \mathbf{M}^{-1} - \frac{k^2}{4} \frac{\mathbf{M}^{-1} \mathbf{g}^n (\mathbf{g}^n)^T \mathbf{M}^{-1}}{1 + \frac{k^2}{4} (\mathbf{g}^n)^T \mathbf{M}^{-1} \mathbf{g}^n} \quad (9)$$

For diagonal \mathbf{M} a linear system solution requires $O(N)$ operations (and for full \mathbf{M} , a linear system involving \mathbf{M}^{-1} must be solved, which is the same as in the case of other algorithms presented [2]).

Example: Nonlinear String Vibration

As a nontrivial example of interest in musical acoustics, consider the case of fully nonlinear string vibration including longitudinal/transverse coupling [12]. This system has been dealt with by various authors, leading to energy-conserving methods relying on nonlinear iterative solvers [13], quadratised methods requiring full linear system solution [9] as well as in the recent article by Marazzato et al. [2]. It may be written as the following (nondimensional) coupled system of PDEs:

$$\partial_t^2 u = \partial_x (\partial \mathcal{V} / \partial w_u) \quad \partial_t^2 v = \partial_x (\partial \mathcal{V} / \partial w_v) \quad w_u = \partial_x u \quad w_v = \partial_x v \quad (10)$$

Here, $u(x, t)$ and $v(x, t)$ are the longitudinal and transverse displacement of a string, defined for $x \in [0, 1]$, and $t \geq 0$. ∂_t and ∂_x represent partial differentiation with respect to x and t , respectively.

The potential energy density \mathcal{V} is defined by

$$\mathcal{V}(w_u, w_v) = \frac{1}{2} (w_u^2 + w_v^2) - \alpha \left(\sqrt{(1 + w_u)^2 + w_v^2} - 1 - w_u \right) \quad (11)$$

The complete Hamiltonian for the system is

$$H = \int_0^L \frac{1}{2} (\partial_t u)^2 + \frac{1}{2} (\partial_t v)^2 + \mathcal{V} dx \quad (12)$$

After semidiscretisation (using, e.g., basic finite difference operators to approximate spatial differentiation), a Hamiltonian ODE system of the form of (1) results. Simulation results are presented in Figure 1, under initial conditions of increasing amplitude, and illustrating pseudo-energy conservation to machine accuracy. Calculation time is comparable to that of basic explicit methods (such as, e.g., Störmer). For more details regarding the particular application to the problem of nonlinear string vibration, the reader is referred to the companion paper [4]. A key aspect not discussed here is the possibility of adding an offset, or gauge to the potential energy, which can have a significant ameliorating effect on convergence rates in the resulting numerical implementation. See [4].

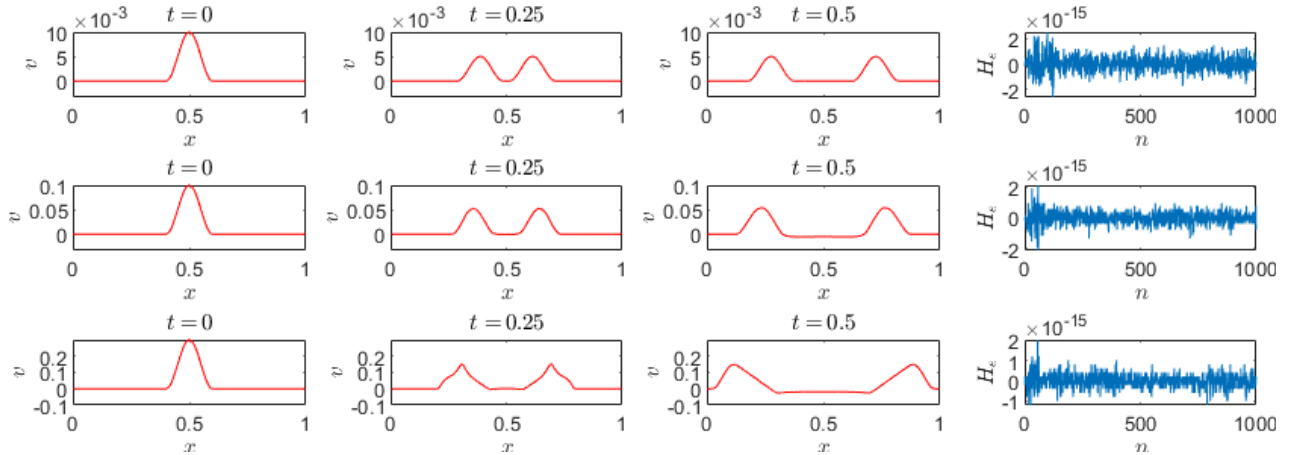


Figure 1: Wave propagation for a pseudo-energy conserving scheme for the nonlinear string system, as defined in (10), with $\alpha = 0.8$, and $k = 10^{-4}$. The string is initialised with zero initial velocity conditions, and with $u = 0$, and with v set to raised cosine distributions of increasing amplitude (top: 0.01, middle: 0.1, bottom; 0.3). At right, the relative energy variation $H_e^n = (H^{n+1/2} - H^{n-1/2}) / H^{1/2}$ is plotted as a function of time step n , showing energy conservation to machine accuracy (approximately 10^{-15}).

Split Forms and Numerical Methods

In some cases, it can be useful to split the potential energy $V(\mathbf{q})$ as

$$V(\mathbf{q}) = V_0(\mathbf{q}) + V'(\mathbf{q}) \quad \text{where} \quad V_0(\mathbf{q}) = \frac{1}{2} \mathbf{q}^T \mathbf{K} \mathbf{q} \quad \text{and} \quad V'(\mathbf{q}) \geq 0 \quad (13)$$

for some positive definite matrix $\mathbf{K} > 0$. While the underlying dynamics are unchanged under such a splitting, it becomes possible to apply different numerical integration techniques to different parts of the problem. In particular, V_0 , a quadratic form, may encapsulate the underlying linear dynamics of a particular system, and V' additional effects due to a nonlinear mechanism.

Under the constraint that $V' \geq 0$, one may write, using $\psi = \sqrt{2V'}$,

$$H(\mathbf{p}, \mathbf{q}) = \frac{1}{2} \mathbf{p}^T \mathbf{M}^{-1} \mathbf{p} + \frac{1}{2} \mathbf{q}^T \mathbf{K} \mathbf{q} + \frac{1}{2} \psi^2 \quad (14)$$

Hamilton's equations may be written as

$$\mathbf{M} \dot{\mathbf{q}} - \mathbf{p} = \mathbf{0} \quad \dot{\mathbf{p}} + \mathbf{K} \mathbf{q} + \psi \mathbf{g} = \mathbf{0} \quad \dot{\psi} = \mathbf{g}^T \dot{\mathbf{q}} \quad (15)$$

where $\mathbf{g} = \nabla \psi$ as before.

Numerical Scheme

Consider the following time-interleaved scheme:

$$\mathbf{q}^{n+1} = \mathbf{q}^n + k \mathbf{M}^{-1} \mathbf{p}^{n+\frac{1}{2}} \quad \mathbf{p}^{n+\frac{1}{2}} = \mathbf{p}^{n-\frac{1}{2}} - k \mathbf{K} \mathbf{q}^{n-\frac{k}{2}} \left(\psi^{n+\frac{1}{2}} + \psi^{n-\frac{1}{2}} \right) \mathbf{g}^n \quad \psi^{n+\frac{1}{2}} = \psi^{n-\frac{1}{2}} + \frac{1}{2} (\mathbf{g}^n)^T (\mathbf{q}^{n+1} - \mathbf{q}^{n-1}) \quad (16)$$

The update follows, from the extension of (8), as

$$\mathbf{A}^n \mathbf{q}^{n+1} = \mathbf{b}^n \quad \mathbf{A}^n = \mathbf{M} + \frac{k^2}{4} \mathbf{g}^n (\mathbf{g}^n)^T \quad \mathbf{b}^n = (2\mathbf{M} - k^2 \mathbf{K}) \mathbf{q}^n - k^2 \mathbf{g}^n \psi^{n-\frac{1}{2}} - \left(\mathbf{M} - \frac{k^2}{4} \mathbf{g}^n (\mathbf{g}^n)^T \right) \mathbf{q}^{n-1} \quad (17)$$

and again, a fast implementation is possible using Sherman Morrison, through the explicit inversion of \mathbf{A}^n .

This scheme now possesses the conserved numerical energy:

$$H^{n+\frac{1}{2}} = \frac{1}{2} \left(\mathbf{p}^{n+\frac{1}{2}} \right)^T \mathbf{M}^{-1} \mathbf{p}^{n+\frac{1}{2}} + \frac{1}{2} (\mathbf{q}^{n+1})^T \mathbf{K} \mathbf{q}^n + \frac{1}{2} \left(\psi^{n+\frac{1}{2}} \right)^2 = \text{constant} \quad (18)$$

This expression, though conserved, is of indefinite sign, due to the second term. However, this term may be bounded as

$$\frac{1}{2} (\mathbf{q}^{n+1})^T \mathbf{K} \mathbf{q}^n \geq -\frac{1}{8} (\mathbf{q}^{n+1} - \mathbf{q}^n)^T \mathbf{K} (\mathbf{q}^{n+1} - \mathbf{q}^n) = -\frac{k^2}{8} \left(\mathbf{p}^{n+\frac{1}{2}} \right)^T \mathbf{M}^{-1} \mathbf{K} \mathbf{M}^{-1} \mathbf{p}^{n+\frac{1}{2}} \quad (19)$$

and thus

$$H^{n+\frac{1}{2}} \geq \frac{1}{2} \left(\mathbf{p}^{n+\frac{1}{2}} \right)^T \left(\mathbf{M}^{-1} - \frac{k^2}{4} \mathbf{M}^{-1} \mathbf{K} \mathbf{M}^{-1} \right) \mathbf{p}^{n+\frac{1}{2}} + \frac{1}{2} \left(\psi^{n+\frac{1}{2}} \right)^2 \quad (20)$$

A condition for non-negativity then follows as

$$k \leq \frac{2}{\lambda_{\max} \left(\mathbf{M}^{-\frac{1}{2}} \mathbf{K} \mathbf{M}^{-\frac{1}{2}} \right)} \quad (21)$$

where $\mathbf{M}^{\frac{1}{2}}$ is the positive matrix square root of the diagonal matrix \mathbf{M} . (If \mathbf{M} is not diagonal, but still positive definite, then the condition above may be generalized to include the unique triangular factors of \mathbf{M} .) This serves as a numerical stability condition for scheme (16). Notice that the scheme is now conditionally stable, but the stability condition depends only on the linear dynamics, and is independent of the nonlinearity. This scheme is distinct from (5), which is unconditionally stable. Indeed, beyond these two choices a family of conservative conditionally stable methods is available, depending on how the splitting of the potential energy V is carried out.

Example: The Föppl-von Kármán Equations

Consider a flat, thin plate, of thickness ξ in m, and of material characterised by Young's modulus E , in Pa, density ρ , in $\text{kg} \cdot \text{m}^{-3}$, and Poisson's ratio ν . The plate is assumed defined over a region $(x, y) \in \mathcal{D} \in \mathbb{R}^2$, and has displacement $u(x, y, t)$. High amplitude vibration of the plate is described by the The Föppl-von Kármán equations:

$$\rho \xi \Delta \partial_t^2 u = -D \Delta \Delta u + \mathcal{L}(u, F) \quad \frac{2}{E \xi} \Delta \Delta F = -\mathcal{L}(u, u) \quad (22)$$

Here, $D = E \xi^3 / 12(1 - \nu^2)$ is the flexural rigidity for the plate, and $F(x, y, t)$ is the Airy stress function, Δ is the two-dimensional Laplacian operator $\Delta = \partial_x^2 + \partial_y^2$, where ∂_x and ∂_y represent partial differentiation with respect to x and y , respectively. $\Delta \Delta$ is the biharmonic operator. The special bilinear operator \mathcal{L} is defined by

$$\mathcal{L}(f, g) = \partial_x^2 f \partial_y^2 g + \partial_y^2 f \partial_x^2 g - 2 \partial_x \partial_y f \partial_x \partial_y g \quad (23)$$

Two initial conditions, $u(x, y, 0)$ and $\partial_t u|_{x, y, t=0}$ are required; in this paper, boundary conditions are chosen to be simply supported over the boundary $\partial \mathcal{D}$ of \mathcal{D} [14].

The Hamiltonian for this system is given by

$$H = \iint_{\mathcal{D}} \frac{\rho \xi}{2} (\partial_t \xi)^2 + \frac{D}{2} (\Delta u)^2 + \frac{1}{2 E \xi} (\Delta F)^2 d\sigma \quad (24)$$

(Note that this particular form of the Hamiltonian is not the most general, but holds under simply supported conditions. It must be augmented by an additional term in the case of, e.g., free edge conditions.)

Semidiscretization

Consider the simple case of a square plate defined over $(x, y) \in [0, L]^2$, for some plate side length L . Assume also that the displacement $u(x, y, t)$ is approximated over a grid with a grid function $u_{l,m}(t)$ such that

$$u_{l,m}(t) \approx u(x = lh, y = mh, t) \quad l, m = 1, \dots, M - 1 \quad (25)$$

Here, h is the grid spacing, and is chosen such that $h = L/M$, for some integer M . Simply supported conditions are assumed here, so that $u_{l,m}(t) = 0$ for $l, m = 0, M$.

There are many approaches to spatial discretization; the simplest is to make use of basic difference operators of the form:

$$\delta_{x\pm}u_{l,m} = \pm\frac{1}{h}(u_{l\pm 1,m} - u_{l,m}) \quad \delta_{y\pm}u_{l,m} = \pm\frac{1}{h}(u_{l,m\pm 1} - u_{l,m}) \quad (26)$$

which are forward and backward approximations to the spatial derivatives ∂_x and ∂_y , respectively. (Note that the time dependence of $u_{l,m}$ has been suppressed above.) Approximations to the Laplacian and biharmonic operator follow as

$$\delta_{\Delta} = \delta_{x+}\delta_{x-} + \delta_{y+}\delta_{y-} \quad \delta_{\Delta\Delta} = \delta_{\Delta}\delta_{\Delta} \quad (27)$$

A discrete approximation ℓ to the bilinear operator \mathcal{L} may be written, for two grid functions $f_{l,m}, g_{l,m}$, as

$$\begin{aligned} \ell(f, g) = & \delta_{x+}\delta_{x-}f\delta_{y+}\delta_{y-}g + \delta_{y+}\delta_{y-}f\delta_{x+}\delta_{x-}g \\ & -\frac{1}{2}\delta_{x+}\delta_{y+}f\delta_{x+}\delta_{y+}g - \frac{1}{2}\delta_{x+}\delta_{y-}f\delta_{x+}\delta_{y-}g - \frac{1}{2}\delta_{x-}\delta_{y+}f\delta_{x-}\delta_{y+}g - \frac{1}{2}\delta_{x-}\delta_{y-}f\delta_{x-}\delta_{y-}g \end{aligned} \quad (28)$$

A centered second order accurate approximation to (22) follows as

$$\rho\xi\ddot{u}_{l,m} = -D\delta_{\Delta\Delta}u_{l,m} + \ell(u, F) = 0 \quad \frac{2}{E\xi}\delta_{\Delta\Delta}F_{l,m} = -\ell(u, u) \quad (29)$$

It is useful, at this stage, to introduce consolidated vector representations $\mathbf{u}(t)$ and $\mathbf{F}(t)$ of $u_{l,m}(t)$ and $F_{l,m}(t)$; both are $(M-1)^2 \times 1$ column vectors (grid points at the plate edges have been removed here, due to the use of simply supported boundary conditions). All of the difference operators δ above may be replaced by matrix equivalents \mathbf{D} . In particular, $\mathbf{D}_{x-}, \mathbf{D}_{y-}$ are of dimensions $M(M-1) \times (M-1)^2$, $\mathbf{D}_{x+}, \mathbf{D}_{y+}$ are of dimensions $(M-1)^2 \times M(M-1)$, and \mathbf{D}_{Δ} and $\mathbf{D}_{\Delta\Delta}$ are of dimensions $(M-1)^2 \times (M-1)^2$. In this case, simply supported boundary conditions have been taken into account—all matrices are sparse, with $O(M^2)$ nonzero entries.

In this case, (29) can be rewritten as

$$\rho\xi\ddot{\mathbf{u}} = -\mathbf{D}\mathbf{D}_{\Delta\Delta}\mathbf{u} + \ell(\mathbf{u}, \mathbf{F}) = \mathbf{0} \quad \frac{2}{E\xi}\mathbf{D}_{\Delta\Delta}\mathbf{F} = -\ell(\mathbf{u}, \mathbf{u}) \quad (30)$$

To arrive at a first order form (15) in terms of momentum $\mathbf{p} = \mathbf{M}\dot{\mathbf{u}}$ and displacement $\mathbf{q} = \mathbf{u}$, with associated Hamiltonian (14) and energy splitting (13), one may use

$$\mathbf{M} = \rho\xi h^2 \mathbf{I}_{(M-1)^2} \quad \mathbf{K} = Dh^2 \mathbf{D}_{\Delta\Delta} \quad V' = \frac{h^2}{2E\xi} |\mathbf{D}_{\Delta}\mathbf{F}|^2 \quad (31)$$

where here, $\mathbf{I}_{(M-1)^2}$ is the identity matrix of size $(M-1)^2 \times (M-1)^2$.

Fully Discrete Schemes

The most basic scheme for the Föppl-von Kármán system follows from a centered difference approximation to the semi-discrete system of ODEs (30). Introducing the discrete-time vectors \mathbf{u}^n and \mathbf{F}^n , approximating $\mathbf{u}(t)$ and $\mathbf{F}(t)$ at $t = nk$, for integer n and a time step k , the Störmer scheme results as

$$\frac{\rho\xi}{k^2} (\mathbf{u}^{n+1} - 2\mathbf{u}^n + \mathbf{u}^{n-1}) = -\mathbf{D}\mathbf{D}_{\Delta\Delta}\mathbf{u}^n + \ell(\mathbf{u}^n, \mathbf{F}^n) = \mathbf{0} \quad \frac{2}{E\xi}\mathbf{D}_{\Delta\Delta}\mathbf{F}^n = -\ell(\mathbf{u}^n, \mathbf{u}^n) \quad (32)$$

This scheme is simple, but stability is highly dependent on both the choice of time step and on the initial conditions—in general, this scheme will become unstable as the size of the initial condition is increased. The first equation represents the update, and is fully explicit. The second requires the solution of a linear system involving the matrix $\mathbf{D}_{\Delta\Delta}$. As this is of a known form, a Cholesky factorisation may be computed prior to entering the runtime loop, greatly accelerating calculation. This scheme will be referred to as Scheme I subsequently here.

A family of energy-conserving and provably numerically stable schemes has been presented in previous work [15, 14]. Though too elaborate to present in detail here, in its most general form, the update equation is of the form

$$\mathbf{A}^n \mathbf{u}^{n+1} = \mathbf{b}^n \quad (33)$$

where, as in (32), \mathbf{u}^n is the plate displacement in vector form. Here, \mathbf{A}^n and \mathbf{b}^n are a matrix/vector pair which in general are dependent on \mathbf{u}^n and \mathbf{u}^{n-1} ; Although no iterative solvers are required, and thus existence/uniqueness are guaranteed, the linear system to be solved must be constructed anew at each time step, in contrast with (32), and thus compute times are much longer. This scheme will be referred to as Scheme II subsequently here.

Finally, one may employ the fast conservative scheme, as given in (16), and under the choices given in (31). This scheme will be referred to as Scheme III subsequently here. In this case, the scheme is stable under the condition (21) which reduces, in this case, to the following condition on the grid spacing h in terms of the time step k :

$$h \geq h_{\min} = 2\sqrt{k} (D/\rho\xi)^{\frac{1}{4}} \quad (34)$$

Table 1: Timing comparison: Schemes I, II and III for the Föppl-von Kármán System. Run times for 1 s output are given, with time steps k as indicated.

Scheme	$k = 10^{-3}$	$k = 5 \times 10^{-4}$	$k = 10^{-4}$	$k = 5 \times 10^{-5}$	$k = 10^{-5}$
I: Störmer-Verlet	0.032	0.142	0.344	6.04	25.24
II: Energy conserving	0.149	0.636	8.92	327.8	1742.8
III: Fast energy conserving	0.055	0.290	0.593	7.76	31.36

Numerical Results: Föppl-von Kármán Equations

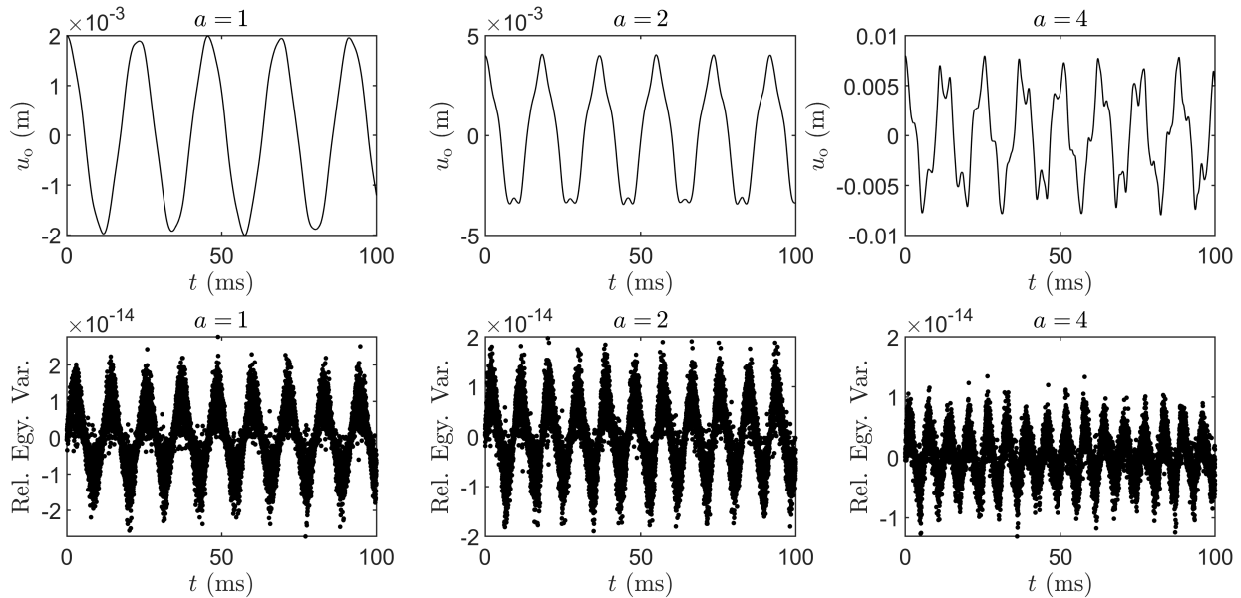
As an example, consider a square plate of side length $L = 0.5$ m, of thickness $\xi = 0.002$ m, and made of steel, with $E = 2 \times 10^{11}$ Pa, $\rho = 7850$ kg·m⁻³, and $\nu = 0.3$. Simply supported boundary conditions are assumed, and the plate is assumed initialised in the lowest linear mode shape, and with zero transverse velocity, so that

$$u(x, y, 0) = a\xi \sin(\pi x/L) \sin(\pi y/L) \quad \partial_t u|_{x,y,t=0} = 0 \quad (35)$$

for some non-dimensional amplitude a . See Figure 2, illustrating plate displacement u_o at the plate center as a function of time, as well as the relative numerical energy variation H_e , defined as

$$H_e^{n+\frac{1}{2}} = \frac{H^{n+\frac{1}{2}} - H^{\frac{1}{2}}}{H^{\frac{1}{2}}} \quad (36)$$

The time step is chosen as $k = 10^{-4}$ s. In all cases, the relative energy variation is on the order of machine accuracy in double precision floating point arithmetic. See also figure 3, illustrating convergence of computed waveforms to trusted high accuracy solutions generated using the standard Scheme I (Störmer) with a very small time step.


 Figure 2: Top row: plate displacement at the plate center, as a function of time, for different initial condition amplitudes $a = 1$, $a = 2$ and $a = 4$. Bottom row: relative numerical energy variation H_e , as defined in (36).

In Table 1 timings per second output are given, for the plate with parameters as described above, and using different time steps k as indicated. All computations were performed in Matlab on a Lenovo P50 laptop on a Xeon E3. Timings are given for the basic Störmer method (Scheme I), the stable energy conserving method as given in [15] (Scheme II) and the new stable energy conserving method presented here (Scheme III). As is clearly evident, the new method performs nearly on par with Störmer, in cases where Störmer is stable—recall that this scheme has obscure stability properties that are highly dependent on the initialisation. These results were computed with initial condition (35) with $a = 4$; at higher amplitudes, Störmer exhibits instability at larger time steps.

Concluding Remarks

A fully explicit method for Hamiltonian numerical integration has been presented here, with a pseudo-energy conservation property leading to unconditional numerical stability—it is different in character from other explicit methods presented

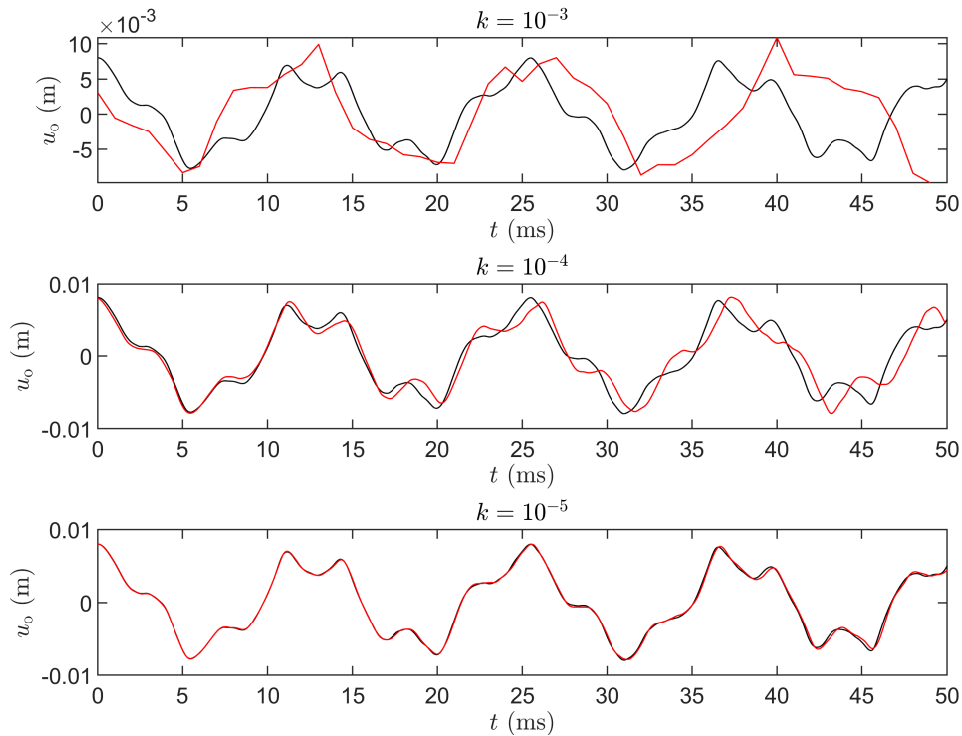


Figure 3: Computed waveforms at the plate center, using scheme III (in red) at different choices of time step k as indicated. Here, a high initial condition amplitude of $a = 4$ is chosen. For reference, a high accuracy solution is computed using Scheme I (Störmer) using a small time step of $k = 10^{-6}$ s, and is shown in black.

recently, in that an additional update is required for the root-potential energy, which is treated as a new independent variable. An extension to the case of split potential forms is also presented, useful in arriving at conditionally stable numerical methods.

The fully explicit character of the eventual update follows from the exploitation of matrix structure, and leads to large increases in computational speed relative to other provably stable energy conserving methods. The method on the whole is nearly as efficient as the simplest explicit schemes for Hamiltonian integration.

Acknowledgments

This work was supported by the European Research Council (ERC), under grant 2020-StG-950084-NEMUS.

References

- [1] E. Hairer, C. Lubich, and G. Wanner, *Geometric Numerical Integration*, Springer Series in Computational Mathematics, 2006.
- [2] F. Marazzato, A. Ern, C. Mariotti, and L. Monasse, “An explicit pseudo-energy conserving time-integration scheme for Hamiltonian dynamics,” *Comp. Methods Appl. Mech. Eng.*, vol. 347, pp. 906–927, 2019.
- [3] J. Shen, J. Xu, and J. Yang, “The scalar auxiliary variable (sav) approach for gradient flows,” *J. Comput. Phys.*, vol. 353, pp. 407–416, 2018.
- [4] M. Ducceschi, S. Bilbao, and Craig J. Webb, “Real-time simulation of the struck piano string with geometrically exact nonlinearity via a scalar quadratic energy method,” in *Proceedings of the European Nonlinear Dynamics Conference*, Lyon, France, July 2022.
- [5] H. Goldstein, C. Poole, and J. Safko, *Classical Mechanics*, Pearson, 2001.
- [6] N. Lopes, T. Hélie, and A. Falaize, “Explicit second-order accurate method for the passive guaranteed simulation of port-hamiltonian systems,” in *Proc. 5th IFAC 2015*, Lyon, France, July 2015.
- [7] A. Falaize, *Modélisation, simulation, génération de code et correction de systèmes multi-physiques audios: Approche par réseau de composants et formulation Hamiltonienne À Ports*, Ph.D. thesis, Université Pierre et Marie Curie, Paris, July 2016.
- [8] M. Ducceschi and S. Bilbao, “Non-iterative solvers for nonlinear problems: the case of collisions,” in *Proc. DAFX*, Birmingham, UK, 2019.
- [9] M. Ducceschi and S. Bilbao, “Non-iterative, conservative schemes for geometrically exact nonlinear string vibration,” in *Proc. ICA*, Aachen, Germany, September 2019.
- [10] X. Yang, “Linear and unconditionally energy stable schemes for the binary fluid-surfactant phase field model,” *Comp. Methods Appl. Mech. Eng.*, vol. 318, pp. 1005–1029, 2017.
- [11] J. Sherman and W. Morrison, “Adjustment of an inverse matrix corresponding to a change in one element of a given matrix,” *Annals of Mathematical Statistics*, vol. 21, no. 1, pp. 124–127, 1950.
- [12] P. Morse and U. Ingard, *Theoretical Acoustics*, Princeton University Press, Princeton, New Jersey, 1968.
- [13] J. Chabassier and P. Joly, “Energy preserving schemes for nonlinear Hamiltonian systems of wave equations: Application to the vibrating piano string,” *Comp. Methods Appl. Mech. Eng.*, vol. 199, no. 45, pp. 2779–2795, 2010.
- [14] S. Bilbao, *Numerical Sound Synthesis*, John Wiley and Sons, Chichester, UK, 2009.
- [15] S. Bilbao, “A family of conservative finite difference schemes for the dynamical von Kármán plate equations,” *Numerical Methods for Partial Differential Equations*, vol. 24, no. 1, pp. 193–216, 2008.